ELSEVIER

J. Construct. Steel Research 31 (1994) 169–186

0143-974X/94/$7.00

Strength Design Curves for Thin-Walled Sections Undergoing Distortional Buckling

Gregory J. Hancock,[a] Young B. Kwon[b] & E. Stefan Bernard[a]

[a]Centre for Advanced Structural Engineering, School of Civil and Mining Engineering, University of Sydney, Sydney, Australia, NSW 2006
[b]Department of Civil Engineering, Yeungnam University, South Korea

(Received 5 January 1994)

ABSTRACT

Certain types of cold-formed sections, notably those composed of high-strength steel, some decking sections and racking sections may undergo a mode of buckling called distortional in which edge and intermediate stiffeners are inadequate to prevent lateral movement of the flanges which they support. The existing design methods in current standards and specifications are often not adequate to account for distortional buckling. This paper describes proposed strength design curves for thin-walled sections undergoing distortional buckling.

The design curves are based on testing and the test data base is included in the paper. The influence of local buckling on distortional buckling is also discussed.

NOTATION

A	Gross section area
A_e	Effective part of gross section area
b	Plate width
b_e	Effective part of plate width
F_y	Yield stress used in design
M_u	Ultimate moment capacity
M_y	Moment at first yield
Z	Gross section modulus
Z_e	Effective section modulus
σ_{de}	Elastic distortional buckling stress
σ_{di}	Inelastic distortional buckling stress

σ_{le} Elastic local buckling stress
σ_m Test maximum strength (ultimate load/gross area)
σ_{max} Maximum design stress
σ_y Test yield stress

1 INTRODUCTION

A mode of failure of thin-walled sections in compression and bending, in which edge-stiffened flange elements of the sections deform by rotation of the flange about the flange–web junction, or where the intermediate stiffener in a flange moves normal to the flange, may occur in sections composed of high-strength steel. This mode of failure has been called distortional buckling. The distortional mode of buckling occurs at longer wavelengths than local buckling and involves membrane displacements of the edge or intermediate stiffeners forming the section. The distortional buckling modes are shown for a rack section in compression, a channel section in compression, a trapezoidal deck in bending and a Z-section in bending in Figs 1(a), (b), (c) and (d) respectively.

Research into the distortional mode of buckling has attracted considerable attention in recent years. Distortional buckling in steel storage rack sections was first discussed by Hancock,[1] where simple design charts for computing the buckling stress were presented. Further research including testing by Lau and Hancock [2–4] resulted in a preliminary set of design

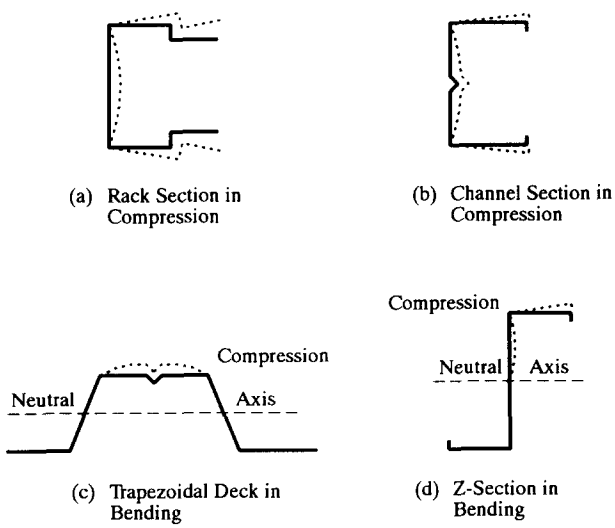

Fig. 1. Distortional buckling modes.

curves based on the Johnston parabola[5] for distortional buckling. These design charts and curves have recently been incorporated in the Australian Steel Storage Rack Standard (Standards Association of Australia[6]). Simplified formulae for computing the elastic distortional buckling stress of sections with edge-stiffened elements were also provided by Lau and Hancock.[7] Charnvarnichborikarn and Polyzois[8] have modified the formulae for elastic buckling to predict the distortional buckling stress of Z-section columns. They have used the same design curves as proposed by Lau and Hancock.[2] Their method accurately predicted the distortional buckling strength of Z-section columns in compression. In neither the method of Lau and Hancock, nor in that of Charnvarnichborikarn and Polyzois, is allowance made for the postbuckling reserve of strength in the distortional mode.

Early work on the distortional buckling mode in edge-stiffened elements and intermediate stiffened elements was performed by Desmond, Peköz and Winter.[9,10] In these two papers the buckling mode was given the name 'stiffener buckling mode' in cases where the stiffener was not adequate to prevent its deformation in a plane normal to the element which it supported. This is the same mode of buckling referred to as distortional buckling in this paper. The design methods proposed for edge and intermediate stiffened elements by Desmond, Peköz and Winter have been incorporated in the AISI Specification.[11] They account for the inability of the stiffener to prevent distortional buckling by reducing the local buckling coefficient for the plate element supported by the stiffener below 4·0 and then including this reduced buckling coefficient in the Winter effective width formula used to compute the strength of the plate element. The design methods do not account for the restraint to distortional buckling provided by the web of the section. The use of the Winter effective width formula allows for postbuckling in the distortional mode. However, as discussed in Kwon and Hancock,[12] the design method in the AISI Specification is unconservative for distortional buckling of channel sections composed of high-strength steel of yield stress 550 MPa, and so alternative design methods are necessary to design against distortional buckling in this case.

An alternative approach has been to account for the distortional mode of buckling of edge and intermediate stiffeners as a compressed strut on an elastic foundation where the elastic foundation is represented by a spring which depends upon the bending stiffness of adjacent parts of plane elements and on the boundary conditions of the element. This procedure has been adopted in Eurocode 3 Part 1.3.[13] The design strength of the stiffener is based upon the conventional compression member design curve in the Eurocode with $\alpha = 0{\cdot}13$. The method accounts for the elastic

restraint of all elements in the section including the web by incorporation of their flexibility in the elastic spring restraint. However, the method does not allow for any postbuckling reserve in the distortional buckling mode. A detailed discussion of this method applied to channel sections is given in Buhagiar, Chapman and Dowling.[14]

A related problem is that of the buckling of the unsupported compression flanges of panel beams (decks with vertical upstands used to provide interlocking between adjacent panels). The distortional buckling mode involves rotation of the web–flange element about the axis of the web and tension flange. A design procedure for this type of distortional buckling has been provided by Serrette and Peköz.[15] The method is based on the elastic buckling stress of the compression flange computed using formulae for the flexural–torsional buckling of the web–flange element elastically restrained by the tension flange. The strength design curve is the Johnston parabola as used by Lau and Hancock[2] and Charnvarnichborikarn and Polyzois.[8] The method does not allow for postbuckling in the distortional mode, although allowance is made for the interaction of local and distortional buckling.

The purpose of this paper is to compare two different sets of design curves which have been proposed for distortional buckling and which are applicable for sections buckling in the distortional mode with the test results performed on a range of sections at the University of Sydney. The design methods are applicable to sections subjected to compression or bending, and can account for sections which buckle in the distortional mode interacting with the local mode.

2 TEST RESULTS

A detailed test programme on a range of thin-walled cold-formed steel sections has been performed at the University of Sydney to determine the strength of sections failing in the pure distortional buckling mode, or the distortional buckling mode interacting with local buckling (mixed mode). The results of the tests are described for hat, channel and storage rack sections with yield stress in the range 200–480 MPa in Lau and Hancock,[2–4] for channel sections with and without intermediate web stiffeners with yield stress in the range 585–640 MPa by Kwon and Hancock[12,16] for trapezoidal decking sections with intermediate stiffeners and yield stress 650 MPa by Bernard, Bridge and Hancock[17–19], and for Z-sections in bending with yield stress 450 MPa by Minnett[20] and O'Dey.[21]

The tests by Lau and Hancock[2–4] were performed on sections for which the distortional buckling stress was greater than half the yield stress and so

no substantial postbuckling reserve was observed. However, the tests by Kwon and Hancock[12,16] and by Bernard, Bridge and Hancock[17-19] were performed on sections for which the yield stress was significantly higher than the distortional buckling stress and so a substantial postbuckling reserve of strength occurred. The tests by Minnett[20] and O'Dey[21] were performed for sections for which the distortional buckling stress was approximately half the yield stress and so failure occurred at approximately the distortional buckling stress.

The complete set of test results for the channel (CH), rack (RA, RL) and hat (HA) sections shown in Fig. 2 is given in Lau and Hancock[2,4] and is summarised in Table 1, where only those sections which underwent distortional buckling in the tests have been included. The elastic distortional buckling stress (σ_{de}) in Table 1 is based on the spline finite strip analysis accounting for the fixed ends as described in Section 3 below. The yield stress (σ_y) is based on compression coupons. The last number in the specimen nomenclature (e.g. 700 in CH17-700) is the specimen length in mm.

The complete set of test results for the high yield strength channel (CH1, CH2) sections shown in Fig. 3 is given in Kwon and Hancock[12,16] and is summarised in Table 2. The elastic distortional buckling stress (σ_{de}) in Table 2 is based on the spline finite strip analysis accounting for the

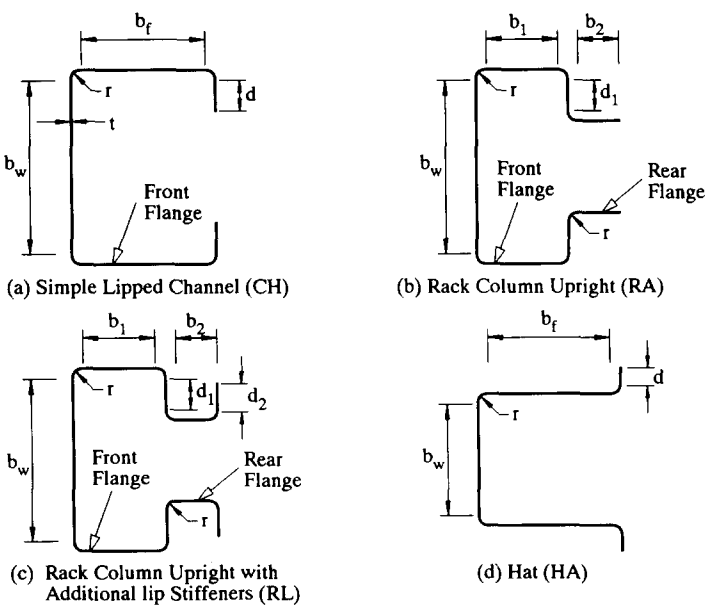

Fig. 2. Lau and Hancock test sections.

TABLE 1
Lau and Hancock Tests (Refs 2–4)

Test section	σ_{de} (*MPa*)	σ_m (*MPa*)	σ_y (*MPa*)	σ_m/σ_y	$\sqrt{\sigma_y/\sigma_{de}}$
CH17-700	307	295	406	0·725	1·15
CH17-1100	308	260	406	0·640	1·15
CH17-1370	308	255	406	0·629	1·15
CH17-1640	300	248	406	0·610	1·16
CH17-1900	295	250	406	0·615	1·17
CH20-700	489	204	217	0·941	0·67
CH24-800	629	403	479	0·841	0·87
CH24-1100	562	375	479	0·783	0·92
RA17-800	404	321	406	0·791	1.00
RA17-1300	349	304	406	0·749	1·08
RA17-1500	343	302	406	0·744	1·09
RA17-1700	324	292	406	0·719	1·12
RA17-1900	316	289	406	0·711	1·13
RA20-800	601	208	217	0·958	0·60
RA20-1300	472	206	217	0·949	0·68
RA24-800	662	413	479	0·862	0·85
RA24-1100	578	382	479	0·797	0·91
RL17-800	322	307	406	0·756	1·12
RL17-1300	320	288	406	0·709	1·13
RL17-1500	320	287	406	0·707	1·13
RL17-1700	321	280	406	0·689	1·12
RL17-1900	315	262	406	0·645	1·14
RL20-800	571	217	217	1·00	0·62
RL24-800	808	410	479	0·856	0·77
RL24-1100	703	394	479	0·823	0·83
HA17-800	278	262	406	0·645	1·21
HA17-1300	270	247	406	0·608	1·23
HA20-800	426	200	217	0·922	0·71
HA24-800	464	341	479	0·712	1·02

fixed ends as described in Section 3 below. The yield stress (σ_y) is based on the 0·2% proof stress of tensile coupons. The second last number in the specimen nomenclature (e.g. 5 in CH1-5-800) is the overall lip depth d in mm, and the last number (e.g. 800) is the specimen length in mm.

The complete set of results for the decking sections (IST, TS3) shown in Fig. 4 is given in Bernard, Bridge and Hancock[17–19] and is summarised in Table 3, where only those IST sections (V-stiffeners) which underwent distortional buckling first or distortional buckling immediately following local buckling are included. The TS3 sections (flat hat stiffeners) which

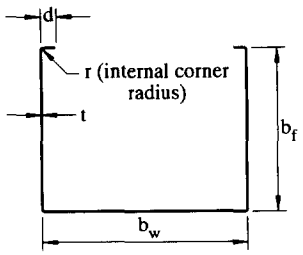

(a) Simple Lipped Channel (CH1)

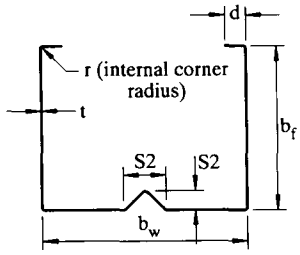

(b) Stiffened Lipped Channel (CH2)

Fig. 3. Kwon and Hancock test sections.

TABLE 2
Kwon and Hancock Tests (Refs 12 and 16)

Test section	σ_{de} (*MPa*)	σ_m (*MPa*)	σ_y (*MPa*)	σ_m/σ_y	$\sqrt{\sigma_y/\sigma_{de}}$
CH1-5-800	46·1	147·8	590	0·251	3·58
CH1-6-800	62·5	147·3	590	0·250	3·07
CH1-7-800	76·1	149·5	590	0·253	2·78
CH1-7-600	81·2	155·7	590	0·264	2·70
CH1-7-400	83·8	160·0	590	0·271	2·65
CH2-7-800	87·0	198·5	590	0·336	2·60
CH2-7-1000	78·3	193·2	590	0·327	2·75
CH2-8-1000	94·9	192·1	590	0·326	2·49
CH2-10-1000	119·8	202·2	590	0·343	2·22
CH2-12-1000	144·6	206·2	590	0·349	2·02
CH2-14-1000	145·4	214·4	590	0·363	2·01

underwent local buckling well before distortional buckling are marked with an asterisk (*). The elastic distortional buckling stress (σ_{de}) was computed using a semi-analytical finite strip analysis as described in Section 3 below. The yield stress (σ_y) is based on the 0·2% proof stress of tensile coupons. The second numeral in the nomenclature for the IST specimens (e.g. 7 in IST 47A) is the approximate stiffener height S in mm.

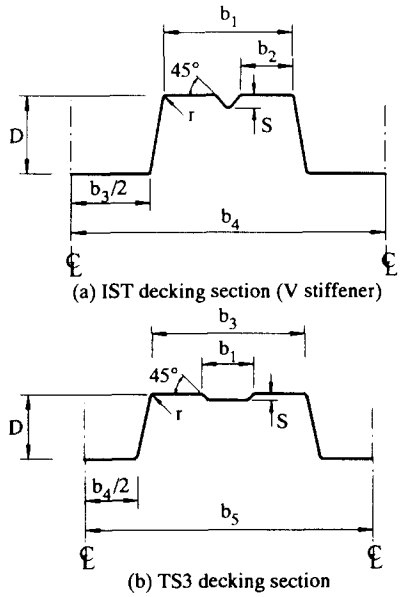

Fig. 4. Bernard, Bridge and Hancock test sections.

TABLE 3
Bernard, Bridge and Hancock Tests (Ref 17–19)

Test section	σ_{de} (*MPa*)	M_u(*test*) (*kN m*)	M_y (*kN m*)	M_u/M_y	$\sqrt{\sigma_y/\sigma_{de}}$
IST 43A	141	3·85	8·92	0·431	2·15
IST 44A	190	4·00	8·88	0·450	1·85
IST 44B	130	3·68	8·95	0·411	2·24
IST 45B	176	3·88	8·90	0·436	1·93
IST 46A	282	4·59	9·26	0·496	1·52
IST 47A	273	4·56	9·01	0·506	1·55
IST 47B	244	4·57	9·06	0·504	1·64
IST 48B	296	4·54	9·14	0·497	1·49
TS3 A1	80	2·96	9·13	0·324	2·86
TS3 A2	104	2·93	9·17	0·320	2·50
TS3 A3	168	2·96	9·01	0·329	1·97
TS3 A4*	260	3·52	8·90	0·396	1·58
TS3 A5*	317	4·10	8·95	0·458	1·44
TS3 A6*	314	3·87	8·90	0·435	1·44
TS3 B4*	231	3·63	8·91	0·407	1·68
TS3 B5*	301	4·01	8·81	0·455	1·47

* Local buckling well before distortional buckling.

TABLE 4
Minnett and O'Dey Tests (Refs 20 and 21)

Test section	σ_{de} (*MPa*)	σ_m (*MPa*)	σ_y (*MPa*)	σ_m/σ_y	$\sqrt{\sigma_y/\sigma_{de}}$
Z20015 N 18	283	302	450	0·67	1·26
Z20015 W 18	262	295	450	0·66	1·31
Z20015 W 15	224	267	450	0·59	1·42
Z20015 W 12	182	245	450	0·54	1·57

The last numeral in the nomenclature for the TS3 specimens (e.g. 6 in TS3 A6) is the approximate stiffener height S in mm.

The complete set of test results for the Z-sections (Z20015) in bending is given in Minnett[20] and O'Dey[21] and is summarised in Table 4. The elastic distortional buckling stress (σ_{de}) was computed using a semi-analytical finite strip method as described in Section 3 below. The yield stress (σ_y) is based on the 0·2% proof stress of tensile coupons. The last number in the nomenclature for the Z20015 specimens (e.g. 15 in Z20015 W 15) is the overall lip depth in mm.

3 CALCULATION OF THE ELASTIC DISTORTIONAL BUCKLING STRESS

A graph of buckling stress versus buckle half-wavelength for a rack section column in compression is shown in Fig. 5. The half-wavelength of the distortional buckling mode at point B is 350 mm whereas the local buckling mode at point A is 65 mm. Overall buckling, including flexural and flexural–torsional buckling where the section remains undistorted, occurs at longer wavelengths. Local buckling involves only plate flexure with the line junctions between intermediate plates remaining straight.

Sections in bending may undergo distortional buckling of two forms, as shown for the channel section in bending in Fig. 6. At point B the mode of buckling is distortional of the same form as that shown at point B in Fig. 5, except that only the compression flange and web participate in the buckling mode for the section in bending. At point C in Fig. 6, distortional buckling occurs where the web bends with a lateral movement of the flange. This type of distortional buckling occurs at much longer half-wavelengths of the order of 2000–10 000 mm. This paper is confined to those forms of distortional buckling of the type shown at point B in Figs 5 and 6. The longer wavelength distortional buckling, which involves

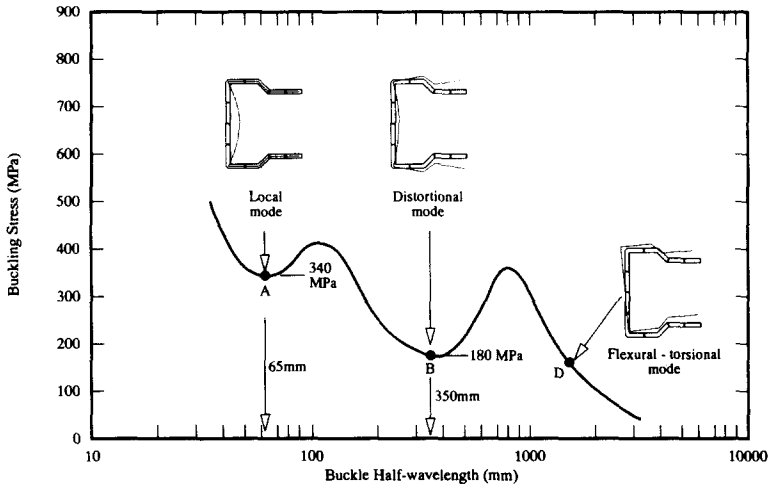

Fig. 5. Rack section column: buckling stress versus half-wavelength.

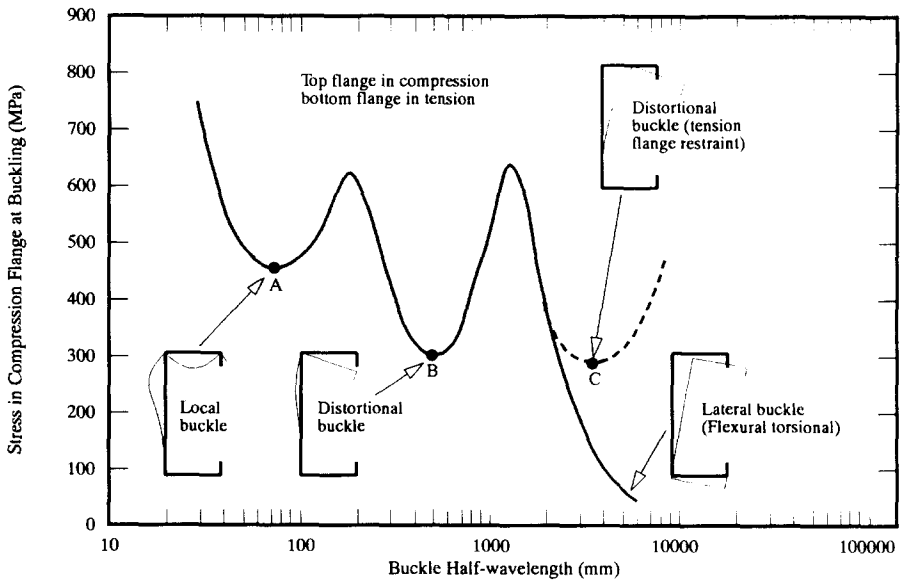

Fig. 6. Channel section: buckling stress versus half-wavelength for major axis bending.

transverse bending of the web, is discussed in more detail in two papers on purlins (Rousch, Rasmussen and Hancock[22] and Trahair[23]).

The design method proposed in Section 4 below requires computation of the elastic distortional buckling stress. The distortional buckling stress

can be calculated using either a computer program based on the finite strip or finite element methods, or analytical formulae specifically determined for distortional buckling. For the sections described in this paper, the distortional buckling stress has been computed using the semi-analytical and spline finite strip methods of buckling analysis (Plank and Wittrick,[24] Lau and Hancock,[25] Hancock[1]). The semi-analytical method assumes simply supported end boundary conditions and is applicable for longer sections where multiple buckle half-waves occur in the section length. It has been used for the trapezoidal decks of Bernard, Bridge and Hancock, and the Z-sections of Minnett and O'Dey. The spline finite strip method is applicable to sections where the end boundary conditions may have an influence such as for sections compressed between rigid end platens. It has been used for the rack sections of Lau and Hancock and the channel sections of Kwon and Hancock. The results of buckling analyses for the CH1 channel section of Kwon and Hancock are shown in Fig. 7, where BFINST denotes the semi-analytical finite strip analysis and BFPLATE denotes the spline finite strip analysis. The BFINST analysis gives the local (σ_{le}) and distortional (σ_{de}) buckling stresses at given half-wavelengths, whereas the BFPLATE analysis gives the actual buckling stress of a given length of section between ends that may be fixed. The abscissa in Fig. 7 for the BFINST analysis indicates one half-wave, whereas for the BFPLATE analysis the abscissa indicates the real column

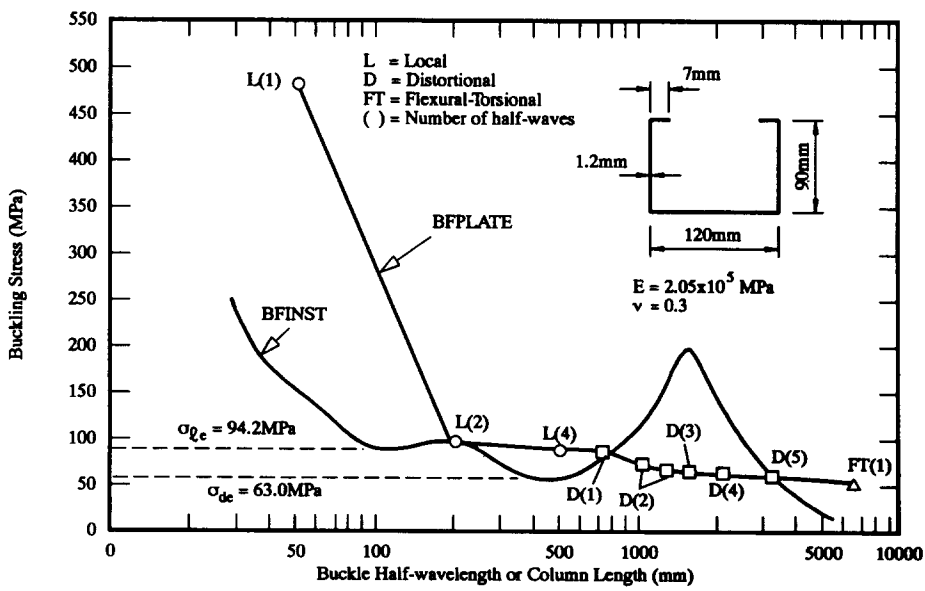

Fig. 7. Finite strip buckling analyses.

length of the section. The different marks indicate local (L), distortional (D) and overall buckling (FT), respectively. It can be observed in Fig. 7 that where the sections buckle in multiple distortional half-waves, the change in the buckling stress in the distortional mode with increasing section length reduces as the effect of the end conditions reduces, and eventually approaches the value produced by the semi-analytical finite strip method.

Simplified design charts have been presented for rack sections in compression by Hancock.[1] For rack, channel and hat sections in compression, simplified formulae for computing the distortional buckling stress of sections with edge-stiffened elements were presented by Lau and Hancock.[7] For Z-sections in compression, formulae for the elastic distortional buckling stress have been given by Charnvarnichborikarn and Polyzois.[8] Formulae for the elastic distortional buckling stress of deck sections in bending are given in Serrette and Peköz.[15] Distortional buckling stresses can be computed approximately using the elastically supported strut model in Eurocode 3 Part 1.3[13] and Buhagiar, Dowling and Chapman.[14]

4 DESIGN FORMULAE

4.1 Effective section approach for distortional buckling

The Winter formula[26] is commonly used in design procedures to determine an estimate of the ultimate load-carrying capacity of plates in compression. In its usual form, it is expressed as

$$\frac{b_e}{b}=\sqrt{\frac{\sigma_{le}}{F_y}}\left(1-0{\cdot}22\sqrt{\frac{\sigma_{le}}{F_y}}\right) \tag{1}$$

where b_e is the effective part of the plate width b, σ_{le} is the elastic local buckling stress and F_y is the yield stress.

Kwon and Hancock[12,16] proposed a modification of this formula to permit application to the distortional mode of buckling for columns undergoing essentially uniform compression. This was done in two stages. At first, the elastic local buckling stress (σ_{le}) was replaced by the elastic distortional buckling stress (σ_{de}) to arrive at

$$\frac{b_e}{b}=1 \qquad \lambda\leqslant 0{\cdot}673 \tag{2a}$$

$$\frac{b_e}{b}=\sqrt{\frac{\sigma_{de}}{F_y}}\left(1-0{\cdot}22\sqrt{\frac{\sigma_{de}}{F_y}}\right) \qquad \lambda\geqslant 0{\cdot}673 \tag{2b}$$

where

$$\lambda = \sqrt{\frac{F_y}{\sigma_{de}}} \tag{2c}$$

In this form, it was assumed that all plate elements forming the cross-section were reduced to effective widths in the same proportions. This was equivalent to

$$\frac{A_e}{A} = \sqrt{\frac{\sigma_{de}}{F_y}}\left(1 - 0{\cdot}22\sqrt{\frac{\sigma_{de}}{F_y}}\right) \tag{3}$$

where A_e is the effective part of the gross section area.

Kwon and Hancock found that this approach yielded unconservative estimates under certain circumstances and thus produced their 'Design Proposal 2' in which the exponent of the (σ_{de}/F_y) term in eqn (2b) was changed from 0·5 to 0·6 and 0·22 coefficient increased to 0·25, thus:

$$\frac{b_e}{b} = 1 \qquad \lambda \leqslant 0{\cdot}561 \tag{4a}$$

$$\frac{b_e}{b} = \left(\frac{\sigma_{de}}{F_y}\right)^{0{\cdot}6}\left(1 - 0{\cdot}25\left(\frac{\sigma_{de}}{F_y}\right)^{0{\cdot}6}\right) \qquad \lambda \geqslant 0{\cdot}561 \tag{4b}$$

where

$$\lambda = \sqrt{\frac{F_y}{\sigma_{de}}} \tag{4c}$$

As for eqn (2), this reduction of the effective widths was performed for all the elements of the section and thus the reduction was equivalent to reducing the gross area (A) to an effective area (A_e).

If a similar approach is applied to members in flexure, then, by direct analogy with eqn (4b), the effective section modulus (Z_e) is calculated as

$$\frac{Z_e}{Z} = \left(\frac{\sigma_{de}}{F_y}\right)^{0{\cdot}6}\left(1 - 0{\cdot}25\left(\frac{\sigma_{de}}{F_y}\right)^{0{\cdot}6}\right) = \frac{\sigma_u}{F_y} \tag{5}$$

leading to the ultimate moment capacity

$$M_u = F_y Z_e = \sigma_u Z \tag{6}$$

where Z is the section modulus of the gross section.

A comparison of eqns (3), (5) and (4b) with the test results is shown in Fig. 8, where the ratios M_u/M_y and σ_m/σ_y are the measured values given in Tables 1–4. The measured face yield stress (σ_y) has been used in the calculation of M_y. In general, eqn (4b) provides a reasonable mean fit to the test results of sections in compression, and eqn (5) provides a reasonable lower bound to the sections in bending, although the trapezoidal deck sections with flat hat stiffeners which underwent local then distortional buckling (solid circles) are predicted unconservatively.

4.2 Maximum stress formulae for distortional buckling

A similar design formula to that used by Chajes *et al.*[27] for inelastic flexural–torsional buckling was adopted for determining the inelastic distortional buckling stress by Lau and Hancock.[2] The proposed formula

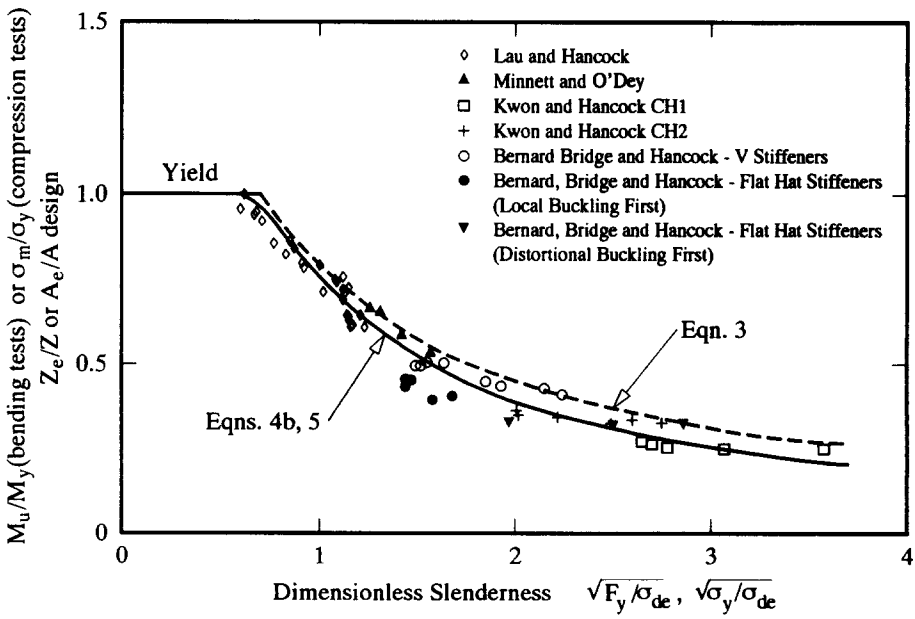

Fig. 8. Comparison of test results with effective section design curves.

is based on the Johnston[5] parabola and is given by

$$\sigma_{di} = F_y\left(1 - \frac{F_y}{4\sigma_{de}}\right) \quad \sigma_{de} \geqslant \frac{F_y}{2} \tag{7a}$$

$$\sigma_{di} = \sigma_{de} \quad \sigma_{de} \leqslant \frac{F_y}{2} \tag{7b}$$

where σ_{de} and σ_{di} are the elastic and inelastic distortional buckling stresses, respectively.

In Kwon and Hancock,[16] an extension of this design curve was proposed for determining the strength of slender sections which are formed from thin steel of high yield strength and which may buckle in the distortional or mixed local–distortional modes in the elastic range of material properties. The proposed formulae for the maximum stress (σ_{max}) (called 'Design Proposal 1' in Kwon and Hancock[16]) are given by

$$\sigma_{max} = F_y\left(1 - \frac{F_y}{4\sigma_{de}}\right) \quad \sigma_{de} \geqslant \frac{F_y}{2} \tag{8a}$$

$$\sigma_{max} = F_y\left(0{\cdot}055\left(\sqrt{\frac{F_y}{\sigma_{de}}} - 3{\cdot}6\right)^2 + 0{\cdot}237\right) \quad \frac{F_y}{13} \leqslant \sigma_{de} \leqslant \frac{F_y}{2} \tag{8b}$$

where σ_{de} is the elastic distortional or mixed mode buckling stress. Equation (8a) is the same as (7a) except that σ_{max} has been substituted for σ_{di}. Equation (8b) is a parabolic fit to the Kwon and Hancock[12,16] test results. A comparison of eqns (8a) and (8b) with the test results in Tables 1–4 is shown in Fig. 9. In general, eqns (8a) and (8b) provide a reasonable mean fit to the test results.

4.3 Influence of local buckling on distortional buckling

Local buckling can occur simultaneously with distortional buckling, or at a higher or lower load. The tests by Kwon and Hancock[12,16] were designed to determine whether adverse interaction occurred if local and distortional buckling were simultaneous or nearly simultaneous. No adverse interaction was found between local and distortional buckling for the channel sections tested, so the distortional buckling strength can be assessed independently of whether local buckling is occurring simultaneously.

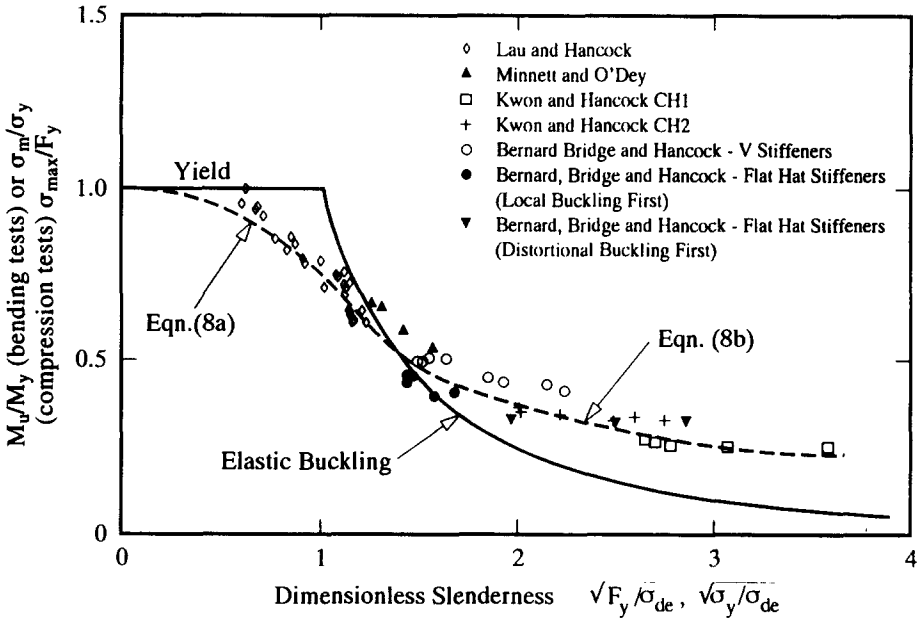

Fig. 9. Comparison of test results with maximum stress design curves.

The tests of trapezoidal decks by Bernard, Bridge and Hancock[17-19] included sections which underwent local buckling before and after distortional buckling. For the sections with V-stiffeners shown by the open circles in Figs 8 and 9, distortional buckling occurring before, or in the approximate vicinity of, local buckling could be predicted using the design formulae proposed for distortional buckling alone. However, sections which underwent local buckling well before distortional buckling needed to be designed using conventional methods to account for local buckling as reported in Bernard, Bridge and Hancock.[17,18] For the sections with flat hat stiffeners shown in Figs 8 and 9 by the solid triangles when distortional buckling occurred first, the design proposals in Sections 4.1 and 4.2 adequately predict the strength of the sections. However, sections which underwent local buckling well before distortional buckling (i.e. $\sigma_{le} < 0{\cdot}85\ \sigma_{de}$), as shown by the solid circles in Figs 8 and 9, could not be predicted conservatively by the formulae in Section 4.1, and a modified effective section method has been proposed by Bernard, Bridge and Hancock.[19]

The modified effective section method involves computing the effective section using conventional methods based on local buckling alone, and then using the maximum stress for distortional buckling as the limiting stress rather than the yield stress. The method allows for postbuckling in the distortional buckling mode.

5 CONCLUSIONS

Two sets of design curves for cold-formed sections undergoing distortional buckling have been proposed and compared with the test results. The first set is based on an effective section approach whilst the second provides a prediction of the maximum stress in the distortional buckling mode including the postbuckling reserve of slender sections. Both approaches were found to produce a reasonable estimate of the results for sections which underwent distortional buckling before or at the same time as local buckling. For sections which undergo local buckling before distortional buckling, a separate method accounting for local buckling should be performed.

ACKNOWLEDGEMENTS

Technical and material support throughout the experimental programme was generously provided by Lysaght Brownbuilt Industries Pty Limited, Colby Engineering Pty Limited and BHP Research, Melbourne Laboratories.

REFERENCES

1. Hancock, G. J., Distortional buckling of steel storage rack columns. *J. Struc. Enging ASCE*, **111** (12) (1985) 2770–83.
2. Lau, S. C. W. & Hancock, G. J., Distortional buckling tests of cold-formed channel sections. *9th International Specialty Conference on Cold-Formed Steel Structures*, St Louis, MO, 1988, pp. 45–73.
3. Lau, S. C. W. & Hancock, G. J., Strength tests and design methods for cold-formed channel columns undergoing distortional buckling. Research Report No. R579, School of Civil and Mining Engineering, University of Sydney, 1988.
4. Lau, S. C. W. & Hancock, G. J., Inelastic buckling of channel columns in the distortional mode. *Thin-Walled Structures*, **10** (1990) 59–84.
5. Johnston, B. G., *Guide to Stability Design Criteria for Metal Structures*, 3rd edn. John Wiley, New York, 1976.
6. Standards Association of Australia, *Steel Storage Racking*, AS4084-1993.
7. Lau, S. C. W. & Hancock, G. J., Distortional buckling formulas for channel columns. *J. Struct. Enging ASCE*, **113** (5) (1987) 1063–78.
8. Charnvarnichborikarn, P. & Polyzois, D., Distortional buckling of cold-formed steel Z-section columns. *11th International Specialty Conference on Cold-Formed Steel Structures*, St Louis, MO, 1992, pp. 353–78.
9. Desmond, T. P., Peköz, T. & Winter, G., Edge stiffeners for thin-walled members. *J. Struct. Enging ASCE*, **107** (2) (1981) 329–53.

10. Desmond, T. P., Peköz, T. & Winter, G., Intermediate stiffeners for thin-walled members. *J. Struct. Enging ASCE*, **107** (4) (1981) 627–48.
11. *Specification for the Design of Cold-Formed Steel Structural Members.* American Iron and Steel Institute, Washington, DC, 1986.
12. Kwon, Y. B. & Hancock, G. J., Design of channels against distortional buckling. *11th International Specialty Conference on Cold-Formed Steel Structures*, St Louis, MO, 1992, pp. 323–52.
13. Eurocode 3, *Cold Formed Thin Gauge Members and Sheeting*, CEN/TC250/SC3-PT 1A, 1992, 3(1.3).
14. Buhagiar, D., Chapman, J. C. & Dowling, P. J., Design of C-sections against deformational lip buckling. *11th International Specialty Conference on Cold-Formed Steel Structures*, St Louis, MO, 1992, pp. 75–94.
15. Serrette, R. & Peköz, T., Local and distortional buckling of thin-walled beams. *11th International Specialty Conference on Cold-Formed Steel Structures*, St Louis, MO, 1992, pp. 63–74.
16. Kwon, Y. B. & Hancock, G. J., Strength tests of cold-formed channel sections undergoing local and distortional buckling. *J. Struct. Enging ASCE*, **117** (2) (1992) 1786–803.
17. Bernard, E. S., Bridge, R. Q. & Hancock, G. J., Tests of profiled steel decks with V-stiffeners. *J. Struct. Enging ACSE*, **119** (1993) 2277–93.
18. Bernard, E. S., Bridge, R. Q. & Hancock, G. J., Tests of profiled steel decks with V-stiffeners. *11th International Specialty Conference on Cold-Formed Steel Structures*, St Louis, MO, 1992, pp. 17–43.
19. Bernard, E. S., Bridge, R. Q. & Hancock, G. J., Intermediate stiffeners in cold-formed profiled steel decks. Part 2: 'Flat hat' shaped stiffeners. Research Report No. R658, School of Civil and Mining Engineering, University of Sydney, 1992.
20. Minnett, A. J., Stiffener buckling of cold-formed steel purlins. Bachelor of Engineering Honours thesis, School of Civil and Mining Engineering, University of Sydney, 1985.
21. O'Dey, N. A., Stiffener buckling of cold-formed steel purlins. Bachelor of Engineering Honours thesis, School of Civil and Mining Engineering, University of Sydney, no date.
22. Rousch, C. J., Rasmussen, K. J. R. & Hancock, G. J., Bending strengths of cold-formed channel and Z sections restrained by sheeting. *Proceedings, International Workshop on Cold-Formed Steel Structures*, Sydney, 1993.
23. Trahair, N. S., Lateral buckling strengths of unsheeted cold-formed beams. *Proceedings, International Workshop on Cold-Formed Steel Structures*, Sydney, 1993.
24. Plank, R. J. & Wittrick, W. H., Buckling under combined loading of thin flat-walled structures by a complex finite strip method. *Int. J. Num. Methods Engng*, **8** (2) (1974) 323–39.
25. Lau, S. C. W. & Hancock, G. J., Buckling of thin flat-walled structures by a spline finite strip method. *Thin-Walled Structures*, **4** (4) (1986) 269–94.
26. Winter, G., Thin-walled structures: theoretical solutions and test results. Preliminary Publication of the 8th Congress, IABSE, 1968, pp. 101–12.
27. Chajes, A., Fang, P. J. & Winter, G., Torsional flexural buckling, elastic and inelastic, of cold formed thin walled columns. Research Bulletin No. 66-1, School of Civil and Mining Engineering, Cornell University, Ithaca, NY, 1966.